Resonance enhancement of two-frequency multiphoton dissociation of HD⁺

Bibhas Dutta,[1] Rangana Bhattacharya,[2] and S. S. Bhattacharyya[2]

[1]*Sambhunath College, Labpur, Birbhum, West Bengal 731 303, India*

[2]*Atomic and Molecular Physics Section, Department of Materials Science, Indian Association for the Cultivation of Science,
Jadavpur, Kolkata 700 032, India*

The angular distribution of photofragments resulting from two-frequency multiphoton dissociation of HD⁺ and their branching ratios to different photon absorption channels have been calculated by the time-independent close-coupling method within the framework of two lowest electronic state model. It is shown that when one of the frequencies, ω_1, is close to an allowed rovibrational transition caused by the permanent dipole moment, the total dissociation linewidth, detailed pattern of angular distribution, and branching ratios to different photon absorption channels vary with the second frequency ω_2. We have varied ω_1 over a narrow range around 11 000 cm^{-1}, which is close to the energy of the $v=0 \to 7$ transition, while ω_2 was varied by about 2500 cm^{-1} up to the dissociation threshold. The branching ratios can be explained in terms of the shape resonances on two different adiabatic potentials caused by the permanent dipole moment and the nonadiabatic couplings with other potentials. Prominent rings in the angular distribution are obtained when the resonance condition is satisfied. They are shown to arise from the mixing of various rotational states due to multiphoton interactions.

I. INTRODUCTION

Multiphoton process in molecules is an intrinsically interesting and rewarding field. Computational studies of intense field molecular multiphoton processes can clarify the basic physics and the role of different interactions in the fundamental steps of such processes. Such information in turn is used to devise schemes of controlling molecular phenomena. In recent past, theoretical and computational studies of interaction of intense field with many small molecules have frequently revealed surprising aspects of molecular processes such as photodissociation, photoionization, photoassociation, and selective rotational excitation. A detailed review of the dynamics of small molecules in very intense fields has been given by Posthumus [1]. Of all these processes, photodissociation of simple molecules, and particularly that of H₂⁺, has been studied most intensively and many new aspects of intense field photodissociation process, such as above-threshold [2] and below-threshold dissociations [3], bond-softening [4], bond-hardening, and vibrational trapping [5], laser induced alignment [6], and zero-photon dissociation [7], have been revealed in the last decade of the 20th century. These results are nontrivial and could not be predicted without detailed numerical computations. However, the simplicity of H₂⁺ (it contains only one electron), and its well known electronic structure, has allowed us to gain a reasonable understanding of multiphoton dissociation of H₂⁺ through extensive computational work. A thorough review of laser-molecule interactions for H₂⁺ with a discussion of the physics involved can be found in [8]. A review focusing on the fundamental processes involved in strong field photodissociation was made in 1995 [9] and a discussion of the works in this field was given by Datta *et al.* [10]. It was established that the gross feature can be explained by a two electronic state approximation. However for very intense fields the high lying electronic states can have important effects on

some aspects of molecular photodissociation at selected intensities and wavelengths [11,12]. In these works the time-independent scattering formalism formulated by Mies and Giusti-Suzor [13] for determining the dissociation linewidth was used. A solution of the time-dependent Schrödinger equation for the study of the dissociation of H₂⁺ has also been made by Barmaki *et al.* [14] using a very large basis set of electronic-vibrational states, many of them above the ionization continuum.

In moderately intense fields, the time-independent close-coupling (c-c) method can be used for the interpretation of laser induced resonance and investigation of possible control scenarios using their interference and overlap. There are also works combining this multiphoton Floquet formalism with Siegert outgoing boundary conditions which permit analysis of the quantal pathways followed by the fragments [15].

As in those earlier works, here also, we have used the time independent close-coupling method for our investigations. The time-independent picture clearly brings out the role of various resonances and it is also possible to study the effect of individual rotational-vibrational states. Short pulses, on the other hand, would excite resonances for which bandwidth of the incident radiation would play a part and we have to disentangle the effects of field induced mixing from the broadband excitation effects. In particular, the dissociation linewidth would contain both the contributions. Thus for very intense pulses at the origin of alignment and/or orientation control scenarios or for dynamical processes involving overlapping resonances, time-dependent methods may be more appropriate. However, the criteria for getting reasonable results through a time-independent calculation have been pointed out earlier [10], and these criteria seem to be satisfied with a pulse length of duration of more than a picosecond for the frequencies used by us.

HD⁺, the isotopic analog of H₂⁺, has also played a key role in strong field molecular dynamics studies. Because of

its heteronuclearity, HD$^+$ has a permanent dipole moment which diverges asymptotically and the dissociation products go to distinct atomic states [16,17]. The question of the importance of the coupling caused by this interaction and its influence on various molecular processes for different field parameters is of major concern in molecular physics. This coupling can be expected to have important consequences as far as dissociation of HD$^+$ in monochromatic [18,19] or bichromatic [20,21] laser field is concerned. However, the various ways in which this interaction can influence the observable characteristics of multiphoton dissociation (MPD) are not as well understood as the dynamics of intense field processes in H$_2^+$ and are now under active investigation both theoretically and experimentally. These characteristics include the total probability of MPD, energy, and angular distribution of the photofragments for different frequencies and intensities as well as pulse duration.

One of the major consequences of the presence of diagonal matrix elements of the electronic dipole moment operator is the possibility of vibrational resonances in IR fields [19–21]. In [19] Kondorskiy and Nakamura demonstrated that the presence of intermediate bound vibrational, rotational states which can be reached by dipole transitions from the initial state can produce photofragment peaks other than those obtained for H$_2^+$ and with different kinds of angular distributions. This phenomenon of intermediate resonance was earlier investigated by us in a different context using a one-dimensional (1D) model of HD$^+$ molecule in a two-frequency field, one of which may cause transition to a bound vibrational level of the ground electronic state [19]. These intermediate resonances were shown to introduce a number of peaks in the spectrum of dissociation linewidth in a two-frequency field when both fields have similar intensities. At frequencies intermediate between the two resonances zero linewidth was also observed. The change in linewidth depends on both the frequencies in a way determined by the distortion of the potential surfaces of the molecules caused by various multiphoton couplings under the joint action of the two fields.

A later three-dimensional treatment, for two-frequency fields, indicated that the laser induced resonances remain recognizable in the multiphoton dissociation spectrum [21]. The branching ratio of the photofragments to channels involving different numbers of net absorbed photons also showed variation with frequencies of the nonresonant field which followed the pattern of variation of the total dissociation linewidth. Intriguing hints of striking change of the photofragment angular distribution and branching ratios around the resonances could also be obtained from these calculations. However, this work, to some extent, destroyed the intuitively easy to understand picture of 1D resonant MPD [20]. The details of the resonance were shown to be nontrivial and further theoretical effort for their full understanding and meaningful correlations with experimental data seemed to be necessary.

In this work we report some further exploration of the same molecular system, i.e., HD$^+$ in a bichromatic field with the objective of gaining a more detailed and basic understanding of the nature of laser induced resonances and interpreting its various features. In particular, we seek possible explanations of the changes of branching ratios and angular distributions in terms of fundamental mechanism such as bond-softening and intermediate shape resonances. As before, we use two linearly polarized electromagnetic waves, each of intensity 1 TW/cm^2, and start from the ground rovibrational level. Apart from confirming our interpretation of the postulated physical mechanism behind resonant multiphoton dissociation, we also show that the enhancement of the linewidths at specific frequencies can be interpreted as being due to shape resonances in an adiabatic potential which is special to HD$^+$ as distinct from H$_2^+$.

In a recent paper, Atabek *et al.* [22] extended the technique of time-independent dissociation linewidths to define time-dependent linewidths for H$_2^+$ in a pulsed field. They demonstrated the existence of shape resonances accommodated in the lower open adiabatic potential in a two channel problem and showed that the Floquet resonances corresponding to several vibrational states have energies similar to these shape resonances at different intensities. At the same time, the existence of zero linewidth resonances was demonstrated and interpreted in terms of Feshbach resonances in the upper closed adiabatic potentials. Energies of some higher Floquet resonances followed the energies of these Feshbach resonances. They argued that their conclusions are robust with respect to the model itself. In this work we interpret the enhancements of the dissociation linewidths obtained by us in terms of shape resonances in an adiabatic potential whose mechanism of formation is different. The zero width resonances obtained earlier by us [20] were interpreted to be due to interference between shape resonances. When a rotational basis is considered the zero width resonances are destroyed. Many rotational channels become involved and interpretation based on interference mechanism between various resonances become difficult to work out.

We also study the angular distribution in the various fragmentation channels in more detail near the resonances and show in terms of the basic mechanisms why the on-resonance angular distribution of the dissociation fragments (with respect to the direction of polarization of the laser field) is different for the different resonances and different channels. This difference is interpreted both in terms of the mixture of various angular momentum states by multiphoton interactions in the radiatively decaying resonance as well as in terms of the motion of nuclei on the adiabatic surfaces. The intermediate resonances with which we are particularly concerned are shown to arise through mixing of a number of rotational levels on the adiabatic surface arising through multiphoton interactions.

Section II gives a bare outline of the theoretical framework and the calculational methods used along with the different parameters considered. Then we discuss the results and give their theoretical interpretation. We finally end with a brief conclusion.

II. FORMULATION

In the c-c method, we expand the field+molecule wave function in the basis of the products of the electronic +rotational states of the molecular system and the photon

number states of the two-mode linearly polarized fields. The two modes are assumed to be independent of one another and the individual states of the basis set are eigenfunction of the Hamiltonian H_0 which includes the electronic motions in the Coulomb field of the clamped nuclei, the rotational motion of the inter nuclear axis, and the Hamiltonian of the two-mode field.

We denote the individual term of the basis set as $|d\rangle$ where d is a collective index containing all the relevant quantum numbers, the index for the electronic state Λ, the rotational quantum number J, and the net number of photons, n_1 and n_2, absorbed from the two modes with total number of photons N_1 and N_2, respectively. This description implies a quantum treatment of the electromagnetic fields. Thus

$$|d\rangle = |\Lambda, J, n_1, n_2\rangle = \Phi_\Lambda(\vec{r}, R) = Y_{J0}(\theta, \varphi)|N_1 - n_1, N_2 - n_2\rangle.$$
$$(1)$$

We have used radiation linearly polarized along the space fixed Z axis for which the selection rule $\Delta M = 0$ is obeyed, where M is the projection of the angular momentum along Z. Since we start with an initial state $J=0$, we always work with $M=0$. It may be mentioned here that since only Σ states are involved, there is no projection of the angular momentum on the molecule fixed z axis. Λ can have the labels GS and ES corresponding to the ground and first excited dissociative electronic states, respectively, of the single electron system HD$^+$. Thus, apart from the GS or ES label, each basis state would also require three more quantum numbers, n_1, n_2, and J, for its complete specification. From now on each basis state will be denoted as GS(n_1, n_2) or ES(n_1, n_2) and the value of J will be mentioned if required.

The basis states $|d\rangle$ are the eigenfunctions of the Hamiltonian H_0 for the noninteracting field-molecule system which includes the field-free Born-Oppenheimer internuclear potentials and the operator for field-free rotation of the rigid molecule in the space fixed frame,

$$H_0|d\rangle = W_d^0(R)|d\rangle \qquad (2)$$

and

$$W_d^0 = V_\Lambda(R) + (\hbar^2/2\mu)J(J+1)/R^2 - n_1\omega_1 - n_2\omega_2, \quad (3)$$

after a shift of the origin of the total energy to a state corresponding to zero photons of the two modes being present and V_Λ is the internuclear potential of the electronic state Λ.

We call these basis states $|d\rangle$ the channel states and we solve the Schrödinger equation

$$H\Psi(n_1, n_1, E, R) = E\Psi(n_1, n_1, E, R) \qquad (4)$$

in this basis for various (shifted) fixed total energies E of the system and the time-independent wave function $\Psi(E)$ for radial motion of the nuclei can be expressed as

$$\Psi(E, R) = \frac{1}{R}\sum_d |d\rangle F_d(R). \qquad (5)$$

Here $F_d(R)$ are the components of the wave function F of radial nuclear motion in the channel state $|d\rangle$.

The total Hamiltonian H of the interacting field+molecule system is given by

$$H = T_R + H_0 + V_{\text{rad}}^{\text{L}}, \qquad (6)$$

where T_R is the radial kinetic energy operator for nuclear motion and $V_{\text{rad}}^{\text{L}}$ is the field-molecule interaction in the length gauge. Thus the radiative interaction and the radial nuclear motion are operators in the Schrödinger equation which couple different electronic+rotational states and photon absorption channels of the noninteracting field-molecule system according to standard selection rules.

Substitution into the Schrödinger equation gives the second-order coupled differential equations for the expansion coefficients F which can be written in compact form as

$$\left[\frac{\partial^2}{\partial R^2} + \frac{2\mu}{\hbar^2}(E - \vec{U})\right]\vec{F} = 0, \qquad (7)$$

where the matrix elements of $\vec{U}$ are given by

$$U'_{dd} = \left(V_\Lambda(R) + \frac{\hbar^2}{2\mu}\frac{J(J+1)}{R^2} - n_1\hbar\omega_1 - n_2\hbar\omega_2\right)$$
$$\times \delta_{\Lambda\Lambda'}\delta_{n_1 n_1'}\delta_{n_2 n_2'} + 1.71 \times 10^{-3} D_{\Lambda\Lambda'}(R)$$
$$\times \sqrt{I[(2J+1)(2J'+1)]}\begin{pmatrix} J' & 1 & J \\ 0 & 0 & 0 \end{pmatrix}^2, \qquad (8)$$

$D_{\Lambda\Lambda'}(R)$ is the radial matrix element of the dipole moment operator between the electronic states Λ and Λ', and I is the constant laser intensity in W/cm^2, and the result is in cm^{-1}. Here we have used the high intensity approximation ($n_1, n_2 \ll N_1, N_2$) for the quantum field to switch over to the semiclassical description of the process in terms of the intensity of the classical field.

Physically our solution should correspond to a half collision. However we use the standard full collision boundary condition for solution of the radial equation. Including only a finite number (N_0) of channel states $|d\rangle$, this set of equations can be solved for a given E using the standard collision boundary conditions on the matrix of the time-independent scattering wave functions $\vec{F}$. The boundary conditions correspond to asymptotic outgoing wave components in all open channels and an incoming wave in the open channel labeled as o. The components of matrix, $F_{co}(R)$ corresponding to the closed channel denoted by c asymptotically go to zero,

$$F_{co}(R) \sim 0,$$

$$R \rightarrow \infty, \qquad (9)$$

and the asymptotic form of the wave function in another outgoing open channel o' corresponding to the same boundary condition is given by

$$F_{o'o}(R) \sim \left(\frac{2\mu}{\pi K_0\hbar^2}\right)[e^{ik_0R}\delta_{o'o} + e^{ik_{o'0}R}S_{o'o}(N,E)]/2iR,$$

$$R \rightarrow \infty, \qquad (10)$$

where S is the $N_0 \times N_0$ unitary scattering matrix.

As described earlier the time-independent probability $P_{oi}(E)$ of the transition i→o for a given total energy E_v can be obtained from the solution vector $\vec{F}$ of the radial equation

[Eq. (7)]. Here i is an initial field-free bound state which corresponds to a specific closed channel c with wave function $\chi_c(R)$ and o is an outgoing wave in another channel labeled by the quantum numbers specified above,

$$P_{oi}(E) = |\langle F_{co}^*(E,R)|\chi_c(R)\rangle|^2. \quad (11)$$

In other words, the overlap between the component of the radial wave function on various channels and the initial wave function in the closed channel gives the transition matrix element for those channels. The total probability of transition to all possible channels $T_i(E) = \Sigma_o P_{o \leftarrow i}(E)$ must eventually reach unity so this provides a check.

The angular distribution of the photofragments from an initial rovibrational level v_i, J_i in the direction θ with respect to the space fixed Z axis, which coincides with the direction of polarization, is given by [23]

$$P_i(\theta, E_0, n_1, n_2) = k \sum_J |(i)^J Y_{J0}^*(\theta, \varphi) T_{J0}(E_0, n_1, n_2|i)|^2, \quad (12)$$

where $T_{J0}(E_0, n_1, n_2)$ is the bound free transition amplitude for n_1 and n_2 photon absorptions at energy E_0.

In sufficiently weak fields for a given initial state the overlap will be appreciable only for a narrow range of the total energy, which corresponds to the field shifted energy of this initial state. The graph of $P_i(E)$ against E now shows a finite width in energy which is caused by the transitions of the molecular system to the dissociative continua. For a simple Lorentzian shape of P against E, we should observe a single exponential decay with a rate proportional to the width. The position of the center of the Lorentzian will give the shift of the initial state under the action of the radiation field(s). However, for intense field the general pattern of the curve may not be a simple Lorentzian or it can have more than one peak and the resulting picture of decay will be more complex. However, for the intensities we have used, there is only one peak and the line shape is Lorentzian.

For solving the time-independent Schrödinger equation [Eq. (4)] we include in the basis all photon numbers with $n_1 + n_2$ (i.e., total number of absorbed photons) less than or equal to 3 in both GS and ES electronic states along with a couple of other photon number states $(-1, 1)$ and $(-1, 2)$ involving stimulated emission of a single photon of frequency ω_1, which have energies close to the absorption channels considered. We take five rotational states to be associated with each of these combinations of (Λ, n_1, n_2). Since the initial state of the system is taken to be $v=0$, $J=0$ and since interaction with a single photon must cause a change in J by ± 1, $J=0, 2, 4, 6,$ and 8 are associated with even values of $n_1 + n_2$, while states with odd values of $n_1 + n_2$ can have the angular momentum quantum numbers of $J=1, 3, 5, 7,$ and 9. This makes the number of states in the basis set equal to 120. Intensities of both fields have been fixed at 1 TW/cm^2 as in our earlier works [20,21]. The lower frequency ω_1 was varied over a narrow range around 11 000 cm^{-1}, keeping ω_2 fixed and then ω_2 was varied from 19 000 cm^{-1} up to the dissociation limit, keeping ω_1 fixed.

III. RESULTS AND DISCUSSION

Since the frequencies of the photons in both fields are below the dissociation threshold, in the lowest order perturbation theory (LOPT) the dissociation by $2\omega_2$ absorption should dominate. Because of the more favorable Franck-Condon factor we can also expect some dissociation through the higher order $3\omega_2$ transition. Again, enhancement of the total transition probability on resonance of ω_1 with a dipole allowed rovibrational transition may be expected but without any significant variation of the linewidth with ω_2, which may be considered not to cause any significant resonance. However, in our case LOPT is not valid and this simplistic picture must be modified. It will be helpful if we give the basic picture of the process before proceeding with the detailed discussion of our results.

The basic process is best understood in terms of the motion of the nuclei on the adiabatic potential surfaces. In Figs. 1(a) and 1(b) we show simplified diagrams of the adiabatic potentials obtained with intensities equal to 10^{12} W/cm^2, $\omega_1 = 11\,000$ cm^{-1} and $\omega_2 = 20\,668$ cm^{-1}, obtained by diagonalizing the potential matrix $\bar{U}$. These adiabatic surfaces can be coupled by the radial kinetic energy operator, whose matrix elements between two different adiabatic potentials provide the nonadiabatic couplings. Since 120 states have been included in the basis set there should be 120 adiabatic potential curves. We have simplified the presentation by showing only the lowest curve from the manifold of rotational states and this results in 24 adiabatic potentials [Fig. 1(b)]. Each curve can be labeled by two indices (n_1, n_2) and by a further label GS or ES at sufficiently large or small distances. At intermediate values of the internuclear distance the curves do not possess such distinct labels. In Fig. 1(a) the presentation has been further simplified by including only a few (n_1, n_2) channels for obtaining the adiabatic curves over a limited range of energy. The most important photon channels in this energy range are $(0,0)$, $(1,0)$, $(2,0)$, $(1,1)$, and $(3,0)$. Near their minima the adiabatic potentials labeled as GS$(0,0)$ and GS$(1,0)$ have almost the character of the unperturbed potentials dressed by the photon energies. Around $3.5a_0$, the adiabatic GS$(1,0)$ potential shows a strong avoided crossing, marked A, because of the radiative interaction between the photon dressed channels GS$(1,0)$ and ES $(1,1)$. This causes a hump in the adiabatic potential. The horizontal line shows the energy of the lowest bound state supported by the adiabatic GS$(0,0)$ potential, which is very close to the ground state energy because near the minimum the adiabatic potential has not been appreciably deformed from its field-free shape. Now, if the lower bound adiabatic potential, labeled GS$(1,0)$, happens to have a resonance at the same energy, then a part of the vibrational wave packet located in the GS$(0,0)$ potential can be transferred to the GS$(1,0)$ potential. The wave packet will spread and finally dissociate through the adiabatic path. In the case shown the resonance will be an over the barrier shape resonance in the GS$(1,0)$ state and hence it will be diffuse. The limiting step should be the transfer of the wave packet on the lower adiabatic potential.

Two points are to be mentioned here. First, if the above barrier resonance energy does not match the eigenenergy of the upper potential, the transfer cannot occur, and the above
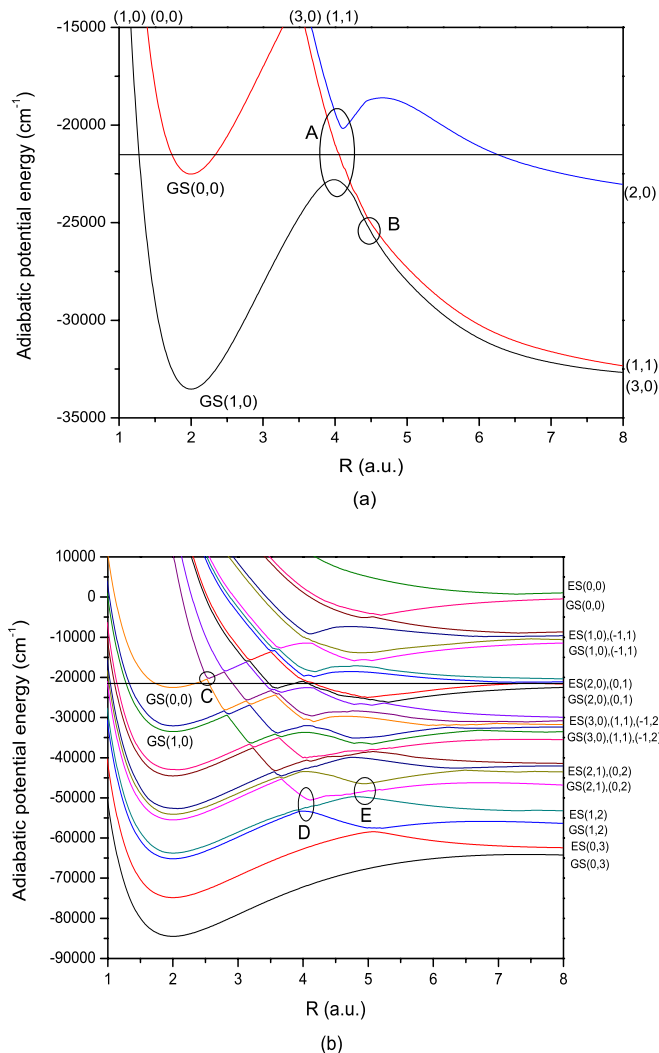
FIG. 1. (a) (Color online) Simplified adiabatic potential energy curves considering the two electronic states GS and ES of HD^+ and drawn for laser frequencies $\omega_1 = 11\,000$ cm^{-1}, $\omega_2 = 20\,668$ cm^{-1} and for each laser having intensity of 1 TW/cm^2. The horizontal line denotes the energy of the shape resonance and on this scale this is almost same as the energy of the initial $v=0$, $J=0$ state. (b) Simplified adiabatic potential energy curves for the same system and same parameters considering only the (0,0), (1,0), (2,0), (1,1), and (3,0) channels not including the rotational splittings. The horizontal line denotes the energy of the shape resonance and of the initial $v=0$, $J=0$ state.

mechanism of dissociation will not be operative. Dissociation would still occur but only through the pathways shown in Fig. 1(b), with smaller rates. Since these pathways will be present in the resonant case also, the matching will cause enhancement of the dissociation linewidth. Second, the adiabatic path along GS(1,0) can only be taken by the system because of its permanent dipole moment. For the isotopic nonpolar counterpart H_2^+, the adiabatic potential GS(1,0) does not exist and there can be no question of resonant enhancement. In fact, this resonance mechanism of two-photon dissociation should be universal for polar molecules if the frequencies are correctly chosen, though for lower values of ω_1 the bond in the adiabatic GS(1,0) state may not be com-

pletely softened and the shape resonance may be of tunneling type and hence sharper. The resonance energies will depend on the exact location and height of the adiabatic potential barrier, which is caused mainly by the radiative interaction through $1\omega_2$ photon coupling with the ES state and should depend on the frequency and intensity of the second field. We may also mention here that for appropriate frequencies and sufficiently high intensities there exists a theoretical possibility of two-photon resonance enhancements of the linewidth. This may involve an adiabatic potential supporting quasibound states caused either by a net two-photon absorption or by a Raman-like process. At our intensities we did not find any signature of Raman-like two-photon resonances in dissociation.

Other feature of the resonant dissociation in this specific case is apparent from Fig. 1(b). Since the energy of the (3,0) channel is quite close to that of the (1,1) channel for the frequencies used here, they interact and in the diagram the adiabatic path from the GS(1,0) potential is shown to lead to the ES(3,0) state at large distances. In practice, following of the adiabatic path near B would require the exchange of a large number of photons between the molecule and the field and the system may prefer to cross over and dissociate through the state which goes to ES(1,1) at large distances. We say that though a fully adiabatic passage should cause a $3\omega_1$ photon absorption, the nonadiabatic coupling between the two close adiabatic states due to the nuclear motion near B would lead to dissociation by (1+1) photon absorption when the resonance conditions are satisfied.

Referring to Fig. 1(b) we see that a bound state supported by the adiabatic potential labeled GS(0,0) can acquire a finite decay width and can become a tunneling type shape resonance because of the presence of the avoided crossing with the ES(0,3) potential at C. Tunneling through the barrier to the repulsive portion of the adiabatic potential amounts to a direct $3\omega_2$ photon absorption. Since in our case the initial state is the ground vibrational state, we need not be concerned with avoided crossings of the GS(0,0) potential at larger distances because the initial wave function will be practically zero at these distances. Once tunneling has occurred, the initial wave packet is accelerated and will mostly follow the diabatic path until it reaches the strongly avoided $1\omega_1$ crossing D near $4a_0$. Further nonadiabatic couplings in the region E would cause a redistribution of the photofragments flux to (1,2) and (0,2) channels. The distribution among the channels and between the GS and ES states will depend on the details of the nonadiabatic interactions (we recall that the differences between the asymptotic energies of some of these channels are very small and the permanent dipole moment becomes quite large). However it is clear that in absence of resonance in the GS(1,0) potential, the shape resonance in the GS(0,0) potential cannot decay to channels such as (3,0), (1,1), etc.

Figure 2 shows our results for the linewidth when we vary the frequency ω_1 in the range of 10 970–11 030 cm^{-1}, keeping ω_2 fixed at two values, 20 668 and 20 900 cm^{-1}. We see that only when $\omega_2 = 20\,668$ cm^{-1} we get a resonance enhancement by varying ω_1, with a maximum for $\omega_1 = 11\,000$ cm^{-1}. We can interpret this as being due to a shape resonance in the GS(1,0) adiabatic potential of Fig. 1(a) for
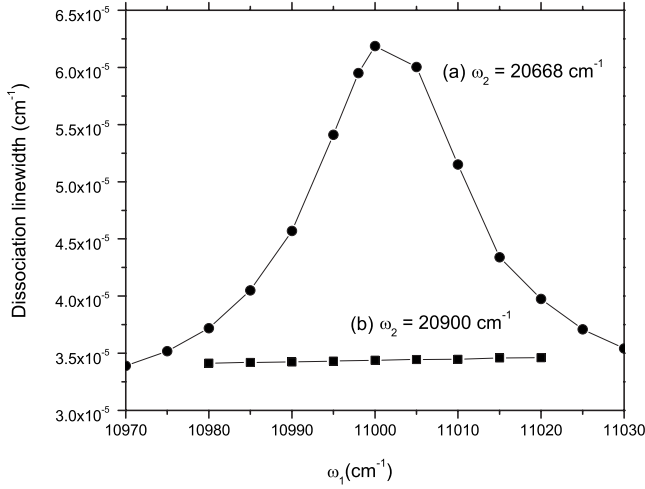
FIG. 2. The total dissociation linewidth of HD$^+$ from the initial level $v_i=0$, $J_i=0$ for field intensities of 1 TW/cm^2 as a function of ω_1 when ω_2 is fixed at (a) 20 668 cm^{-1} and (b) 20 900 cm^{-1}.

this combination of frequencies. Use of a different value of $\omega_2=20\,900$ cm^{-1} does not give any enhancement of the linewidth within the interval of ω_1 studied. This demonstrates the possibility of enhancing or suppressing a resonant dissociative transition by the use of a nonresonant field because an intermediate resonance can be sensitive to the presence of nonresonant fields which modify the adiabatic potentials.

We show in Fig. 3 the variation of dissociation linewidth with ω_2, keeping ω_1 fixed at 11 000 cm^{-1}, the value which gave a peak for a fixed ω_2. Enhancements of the linewidth are found at five different values of ω_2 in the range of 19 500–21 500 cm^{-1}. These peaks in the linewidth are superposed on a background slowly increasing with ω_2 and the maximum increase varies from 50% to 100% of the background value. For the fixed value of ω_1 a resonance in the GS(1,0) adiabatic potential occurs only at these frequencies, as explained earlier. The magnitude and the pattern of variation of the nonresonant background with ω_2 does not change
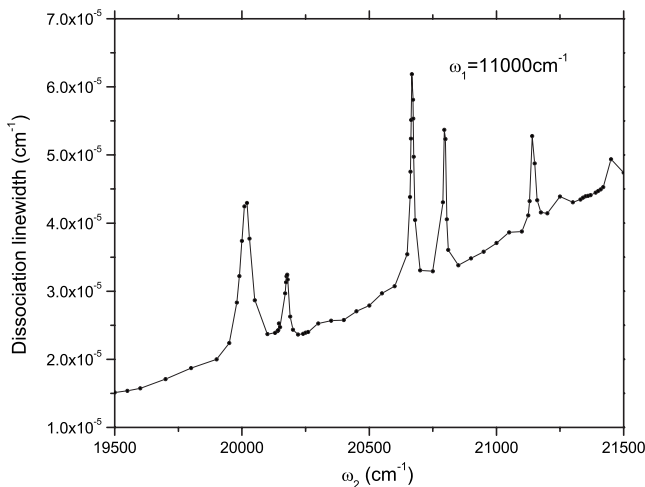

FIG. 3. The total dissociation linewidth of HD$^+$ from the initial level $v_i=0$, $J_i=0$ for field intensities of 1 TW/cm^2 plotted as a function of ω_2 for ω_1 fixed at 11 000 cm^{-1}.
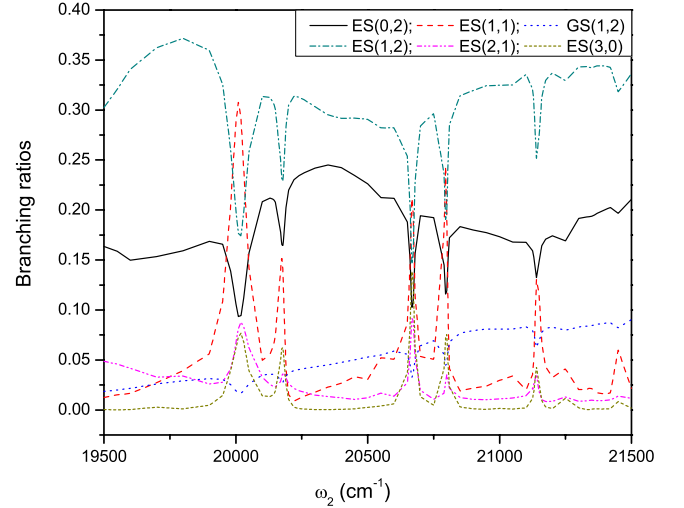

FIG. 4. (Color online) The branching ratios of the photofragments of HD$^+$ to different absorption channels as a function of ω_2 keeping ω_1 fixed at 11 000 cm^{-1} and the two intensities at 10^{12} W/cm^2.

appreciably when we use a different value of ω_1 for obtaining the resonances.

In Fig. 4 we have plotted the branching ratios of the photofragments to different photon absorption channels as functions of the frequency ω_2, keeping ω_1 fixed. We see that at the frequencies ω_2 giving an enhancement of the linewidth, the ES(1,1) channel (corresponding to a net $1\omega_1+1\omega_2$ photon absorption) dominates over other channels. There are also small increases in the branching to ES(2,1) and ES(3,0) channels at those resonant frequencies. However, for frequencies ω_2 away from these values, the major contribution to the dissociation occurs through the ES(1,2) and ES(0,2) and to some extent through GS(1,2) channels. The branching ratios in these channels register sudden drop whenever the resonant frequencies (of ω_2) are approached.

The fragmentation through the (1,1) and to some extent through the (3,0) channels at selected frequencies has been explained through a mechanism involving over the barrier shape resonances in a potential reachable by a single photon absorption and whose positions would depend on both ω_1 and ω_2. If we change ω_1 slightly the coincidence of the resonances with the initial energy is destroyed and no peak in linewidth is observed. However by changing ω_2, the barrier of the adiabatic GS(1,0) potential can be shifted slightly and a shape resonance in the new potential can be brought back into coincidence with that in the GS(0,0) adiabatic potential. For example, we get a peak in the linewidth at $\omega_2=20\,668$ cm^{-1} for $\omega_1=11\,000$ cm^{-1}. This peak is shifted to $\omega_2=20\,681$ cm^{-1} if we change ω_1 to 10 980 cm^{-1} and the same peak occurs for $\omega_2=20\,655$ cm^{-1} when $\omega_1=11\,020$ cm^{-1}. Thus on decreasing ω_1 we must increase ω_2 so that the potential can support a quasibound shape resonance at the same energy. Most of the photofragment flux in all such cases would escape through the ES(1,1) channel. Fully adiabatic passage in the crossing region would also cause transfer to the channel denoted as (3,0). The channel (2,1) has not been shown. The dissociation through the channel also increases at those frequencies.
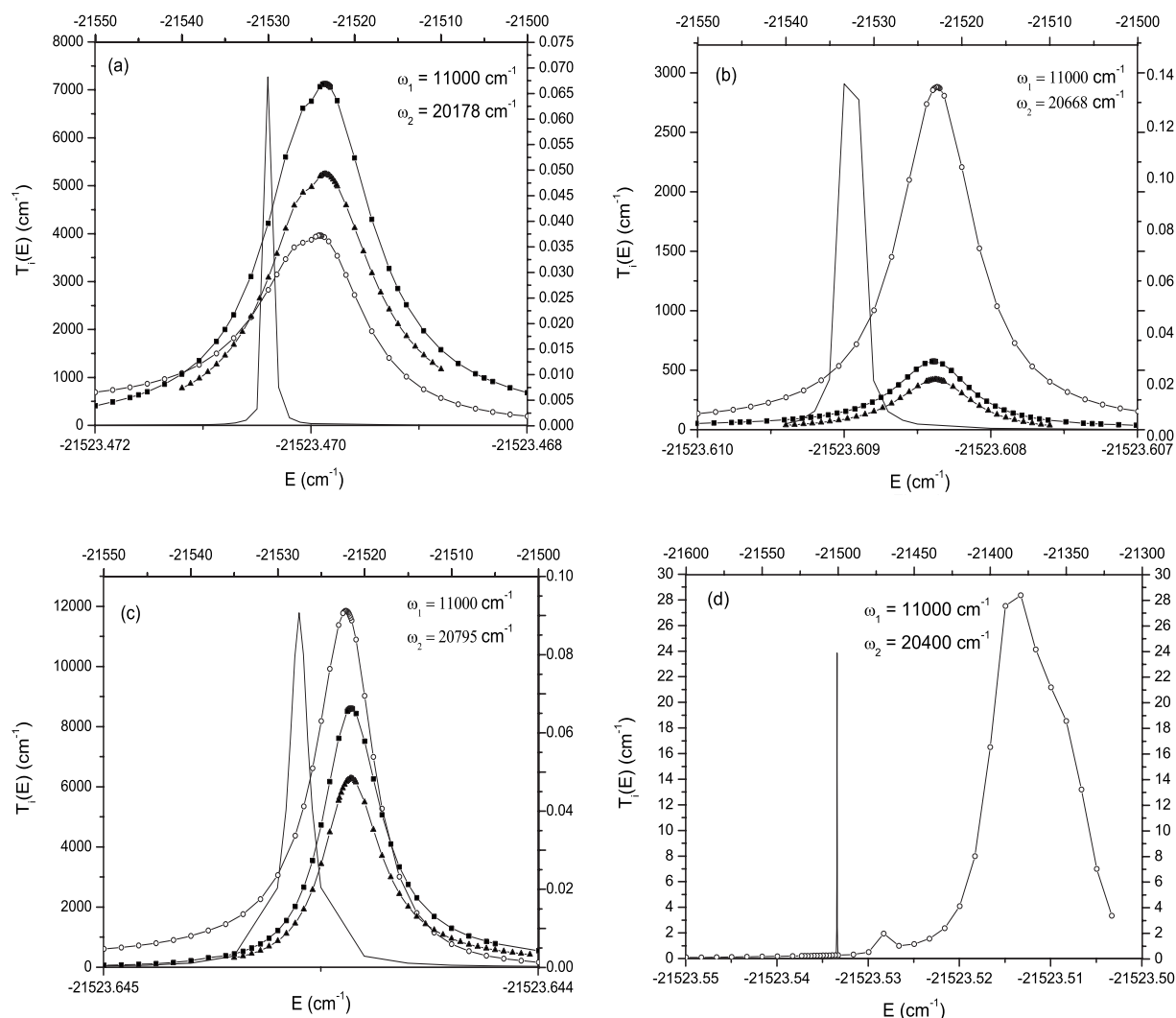
FIG. 5. (a)–(c) The overlaps between different components of the wave function and various bound states (v_i, J_i) are shown as a function of energy for a fixed $\omega_1 = 11\,000$ cm^{-1}. The thin line shows the overlap of $(v_i=0,\ J_i=0)$ with the GS $(n_1=0,\ n_2=0,\ J_i)$ component. The lower and left-hand scales are applicable for this graph. Other curves show the overlaps of $(v_i=7,\ J_i)$ eigenfunctions with the GS $(n_1=1,\ n_2=0,\ J_i)$ components of the scattering wave functions multiplied by appropriate scaling factors. The symbols and multipliers used are the following: $-\bigcirc-\bigcirc-$ overlap with $J_i=1$ and multiplied by 10, $-\blacktriangle-\blacktriangle-$ overlap with $J_i=3$ and multiplied by 50, $-\blacksquare-\blacksquare-$ overlap with $J_i=5$ and multiplied by 50, and the upper and right-hand scales apply for these graphs. (a) $\omega_2 = 20\,178$ cm^{-1}, (b) $\omega_2 = 20\,668$ cm^{-1}, (c) $\omega_2 = 20\,795$ cm^{-1}, and (d) same as above for $\omega_2 = 20\,400$ cm^{-1}. The overlap between $v_i=0, J_i=0$ and the GS $(n_1=0,\ n_2=0,\ J_i)$ component has been multiplied by 10^{-3} and the lower scale applies for this graph. The curve $-\bigcirc-\bigcirc-$ shows the overlap between the eigenfunction $(v_i=7,\ J_i)$ and the component GS $(n_1=1,\ n_2=0,\ J_i=1)$ multiplied by 5000. The upper scale is applicable for this graph.

For a more detailed study of the nature of the resonances, we have calculated the overlap of the scattering wave function with the diabatic rovibrational states corresponding to $v=7$, $J=1,3,5$ in the well supported by the one ω_1 photon dressed GS potential. The squared overlap integrals have been plotted in Figs. 5(a)–5(d). For values of ω_2 giving resonant enhancement of the linewidth, the position in energy of these peaks coincides with those of the overlap between the $n_1=0$, $n_2=0$, $J=0$ component of scattering wave function and the initial eigenstate $v=0$, $J=0$ [Figs. 5(a)–5(c)]. Of course the overlap with the initial state gives very narrow peaks while the peaks of the overlap with $v=7$ state after $1\omega_1$ photon absorption are broad and diffuse. Because of the over the barrier nature of these adiabatic resonances due to the bond softening in this potential, the resonance state decays very fast, in particular through the $1\omega_2$ photon absorption interaction. This requires two scales on both axes for their representations. The essential point is that the peaks occur at the same value of total energy, which signifies that the shape resonance at the GS(1,0) adiabatic potential has a pronounced $v=7$ character for these combinations of frequencies. There is practically no overlap at these energies with any of the $v=6$ or $v=8$ states on this potential and also no signature of resonance with any vibrational state on the corresponding GS(0,1) potential could be found.

At other, nonresonant, frequencies, as shown in Fig. 5(d), peaks of the two overlaps are far apart in energy. This leads to the interpretation that whenever the enhancements of linewidths are seen, they are due to the excitation of a quasiresonant $v=7$ like state in a GS potential after a single ω_1 photon
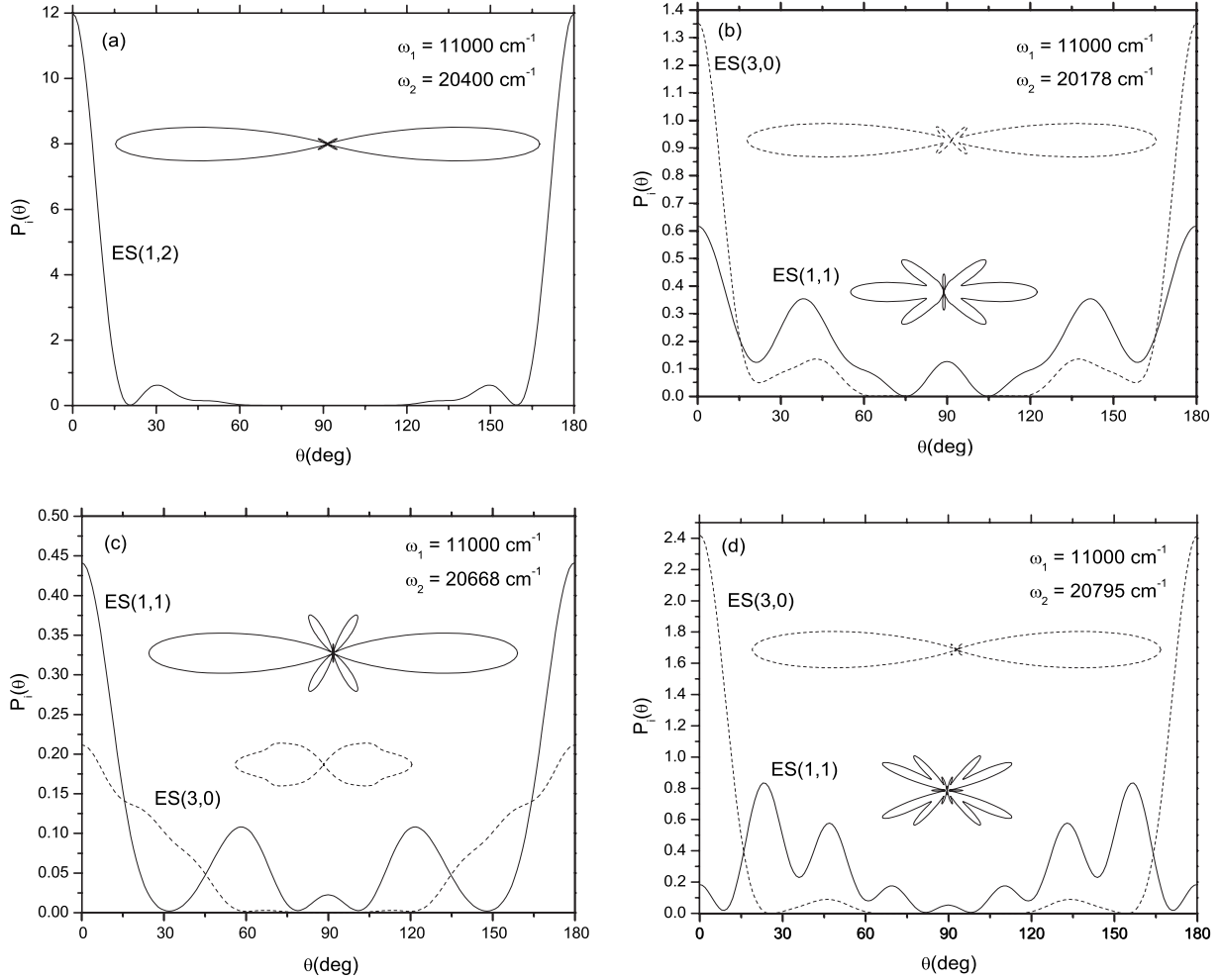
FIG. 6. (a) Angular distribution of the photofragments of HD$^+$ in both Cartesian and polar plots with ω_1 fixed at 11 000 cm^{-1} and two field intensities each of magnitude of 10^{12} W/cm^2 to channel ES(1,2) for nonresonant frequency $\omega_2=20\,400$ cm^{-1}. (b)–(d) Angular distribution of the photofragments of HD$^+$ in both Cartesian and polar plots with ω_1 fixed at 11 000 cm^{-1} and two field intensities each of magnitude of 10^{12} W/cm^2 to channels ES(1,1) and ES(3,0) for resonant frequencies (b) $\omega_2=20\,178$ cm^{-1}, (c) $\omega_2=20\,668$ cm^{-1}, and (d) $\omega_2=20\,795$ cm^{-1}. The solid line corresponds to ES(1,1) and the dashed line corresponds to ES(3,0).

absorption at small values of R. At large R, radiative mixing with other photon number states soon breaks up the molecule. These resonant enhancements in the linewidth are two to three times weaker than those obtained earlier for ω_1 $=100\,053$ cm^{-1} since with this lower value of ω_1, the excited quasiresonance has a $v=6$ character, transitions to which are stronger than those to $v=7$.

From Fig. 5 it is clear that the quasiresonant levels in the GS(1,0) adiabatic potential do not have a pure $J=1$ character but are indeed mixtures of various rotational states. This is because on diagonalization of the potential matrix, radiative transitions to all orders and, in particular, high order stimulated Raman-like transitions to high angular momentum states are included. Hence the adiabatic potentials become superpositions of the channel potentials specified by different J values. Thus each resonant level contains all rotational quantum numbers obeying the symmetry of the interaction. Thus we may conclude that in the limiting step the system is transferred to a mixed angular momentum state in that lower potential containing $J=1,3,5,\ldots$ components. Also, each net photon absorption channel can be reached through various

pathways involving different rotational states (the standard selection rule $\Delta J=\pm 1$ is obeyed for each individual radiative step in the path). The resultant amplitude of transition to a particular channel is the superposition of amplitudes of many such processes involving different numbers of transitions through different angular momentum states. This involvement of different angular momentum states for a particular transition causes a damping of the sharp resonant features obtained in our earlier 1D calculation [20]. However this work, as well as the earlier work [21], shows that the enhancements are damped but not completely washed out when rotations are included.

We have plotted the angular distribution of the photofragments in the dominant channels for both the resonant and nonresonant cases. Figure 6(a) shows the angular distribution pattern for the dominant ES(1,2) channel for a nonresonant frequency combination. The angular distribution consists mainly of narrow cones in the forward and backward directions with respect to the direction of polarization of the laser fields. Such distributions can occur only on mixing of all the (odd) angular momentum states in more or less equal propor-

tions. We may also say that for dissociation through a tunneling resonance, which has its energy below the barrier, the molecules must be well aligned [24].

Figures 6(b)–6(d) show the angular distribution in the (1,1) and (3,0) channels for three cases of intermediate resonance. These channels are reached through excitation of over the barrier shape resonance of the (1,0) potential which has a predominantly $J=1$ character but contains small mixtures of $J=3,5$ and possibly $J=7$ states. A passage from this mixed state to the (1,1) channel through an one-photon absorption would result in an angular pattern which is basically a superposition of P_0 and P_2 polynomials with small mixtures of P_4 and P_6. As the diagrams demonstrate, in many cases there seems to be some mixing of higher angular momentum states in the outgoing wave function in the ES(1,1) channel.

Actually for each combination of n_1 and n_2 there are a number of closely spaced adiabatic potentials with mixed rotational character. A quasibound state with $v=7$ like eigenfunction and eigenenergy equal to that of the shifted $v=0$ state with a dominant $J=1$ character can be excited on one of these GS(1,0) potentials only for particular values of ω_2, but this state is in general different mixtures of angular momentum states for different ω_2 values. After such a resonant state is excited, the dissociaton to the ES(1,1) channel can occur either by a single ω_2 photon absorption or through various multiphoton and Raman-like and nonadiabatic transitions. In general we can expect that, unlike the cases where dissociation occurs through tunneling, there may be quite distinct mixtures of the different partial waves at different frequencies with corresponding variations in the angular pattern. First of all, we note that intermediate resonance for ω_2 $=20\,668$ cm^{-1} is stronger, giving a larger enhancement of linewidth compared to the other resonant frequencies. The angular distribution of the photofragments for this frequency shows distinct lobes which are due to small mixtures of P_4. This seems to be reasonable; for the intermediate resonant $v=7$ like state is mainly of $J=1$ character with a small mixture (about 5%) of $J=3$ and $J=5$ states. This, however, is not the case for wave numbers of 20 178 and 20 795 cm^{-1} where the resonant state has an appreciable $J=5$ rotational character and it is seen that $J=6$ partial waves play important roles. In particular, the elaborate structures of the angular

distribution pattern for 20 795 cm^{-1} may possibly be occurring due to interference of partial waves of the scattering wave functions along the different dissociation paths of the (1,1) channel shown in Fig. 3(b). On the contrary, the angular distribution of the dominant ES(1,1) channel (not shown) of the weak resonances near 21 140 cm^{-1} hardly shows any signature of rotational states higher than P_2 because the resonant state has overwhelmingly $J=1$ character and the higher angular momentum states have not mixed appreciably. Again the angular distribution for $\omega_2=20\,178$ cm^{-1} does show structures which arise due to the presence of higher rotational quantum numbers. Our diagrams also show the angular distribution pattern in the other important channel ES(3,0) on resonance. In this case more radiative interactions may be involved, and the angular distribution does not show in most cases the striking features of the ES(1,1) channel. Indeed, the pattern is intermediate between that for the dominant channels in the off resonance case and the distribution for ES(1,1) channel on resonance.

IV. CONCLUSION

The time-independent close-coupling calculation of two-frequency dissociation of the simplest polar molecule HD$^+$ has once again revealed the importance of permanent dipole induced resonances in determining the photodissociation spectrum and the energy distribution of the photofragments. The transitions due to permanent moments can cause the molecule to follow different adiabatic paths to dissociation which are not possible in the nonpolar isotropic analog H$_2^+$. As the resonant increase of the dissociation linewidth occurs only for selected values of the second nonresonant frequency, the use of a second field allows us to control the kinetic energy and angular distribution of the photofragments to some extent. However, the resonant enhancements are damped by molecular rotations. The gross features of the branching between the various channels at different frequencies can be understood by considering the shape resonance on the two adiabatic potentials. The angular distributions of the products are very different for intermediate resonant and nonresonant cases. In contrast to single frequency dissociation extremely complicated angular distribution patterns can be obtained due to the mixing of rotational states of the resonant level by interaction with the second field.

[1] J. H. Posthumus, Rep. Prog. Phys. **67**, 623 (2004).

[2] A. Giusti-Suzor, X. He, O. Atabek, and F. H. Mies, Phys. Rev. Lett. **64**, 515 (1990).

[3] A. Giusti-Suzor and F. H. Mies, Phys. Rev. Lett. **68**, 3869 (1992).

[4] P. H. Bucksbaum, A. Zavriyev, H. G. Muller, and D. W. Schumacher, Phys. Rev. Lett. **64**, 1883 (1990).

[5] L. J. Frasinski, J. H. Posthumus, J. Plumridge, K. Codling, P. F. Taday, and A. J. Langley, Phys. Rev. Lett. **83**, 3625 (1999).

[6] E. Charron, A. Giusti-Suzor, and F. H. Mies, Phys. Rev. A **49**, R641 (1994).

[7] L. J. Frasinski, J. Plumridge, J. H. Posthumus, K. Codling, P. F. Taday, E. J. Divall, and A. J. Langley, Phys. Rev. Lett. **86**, 2541 (2001).

[8] *Molecules in Intense Laser Fields*, edited by A. D. Bandrauk (Dekker, New York, 1994), Chaps. 2 and 3.

[9] A. Giusti-Suzor, F. H. Mies, L. F. DiMauro, E. Charron, and B. Yang, J. Phys. B **28**, 309 (1995).

[10] A. Datta, S. Saha, and S. S. Bhattacharyya, J. Phys. B **30**, 5737 (1997).

[11] S. Sen, B. Dutta, S. S. Bhattacharyya, and S. Saha, Phys. Rev. A **67**, 053403 (2003).

[12] B. A. Khan, S. Saha, and S. S. Bhattacharyya, Phys. Rev. A **73**, 023423 (2006).

[13] F. H. Mies and A. Giusti-Suzor, Phys. Rev. A **44**, 7547 (1991).

[14] S. Barmaki, H. Bachau, and M. Ghalim, Phys. Rev. A **69**,

043403 (2004).

[15] M. Chrysos, O. Atabek, and R. Lefebvre, Phys. Rev. A **48**, 3845 (1993); **48**, 3855 (1993).

[16] A. Carrington and R. A. Kennedy, Mol. Phys. **56**, 935 (1985).

[17] R. E. Moss and I. A. Sadler, Mol. Phys. **64**, 165 (1988).

[18] E. Charron, A. Giusti-Suzor, and F. H. Mies, J. Chem. Phys. **103**, 7359 (1995).

[19] A. Kondorskiy and H. Nakamura, Phys. Rev. A **66**, 053412 (2002).

[20] A. Datta and S. S. Bhattacharyya, Phys. Rev. A **59**, 4502

(1999).

[21] B. Dutta, S. Sen, S. Saha, and S. S. Bhattacharyya, Phys. Rev. A **68**, 013401 (2003).

[22] O. Atabek, R. Lefebvre, C. Lefebvre, and T. T. Nguyen-Dang, Phys. Rev. A **77**, 043413 (2008).

[23] G. G. Balint-Kurti and M. Shapiro, Adv. Chem. Phys. **60**, 403 (1985).

[24] V. Serov, A. Keller, O. Atabek, H. Figger, and D. Pavicic, Phys. Rev. A **72**, 033413 (2005).